

# Disease contagion models coupled to crowd motion and mesh-free simulation

Parveena Shamim Abdul Salam

Department of Mathematics, TU Kaiserslautern  
Kaiserslautern, 67663, Germany  
parveena@mathematik.uni-kl.de

Wolfgang Bock

Department of Mathematics, TU Kaiserslautern  
Kaiserslautern, 67663, Germany  
bock@mathematik.uni-kl.de

Department of Mathematics, TU Kaiserslautern  
Kaiserslautern, 67663, Germany  
klar@mathematik.uni-kl.de

Department of Mathematics, TU Kaiserslautern  
Kaiserslautern, 67663, Germany  
tiwari@mathematik.uni-kl.de

December 30, 2021

## Abstract

Modeling and simulation of disease spreading in pedestrian crowds has been recently become a topic of increasing relevance. In this paper, we consider the influence of the crowd motion in a complex dynamical environment on the course of infection of the pedestrians. To model the pedestrian dynamics we consider a kinetic equation for multi-group pedestrian flow based on a social force model coupled with

an Eikonal equation. This model is coupled with a non-local SEIS contagion model for disease spread, where besides the description of local contacts also the influence of contact times has been modelled. Hydrodynamic approximations of the coupled system are derived. Finally, simulations of the hydrodynamic model are carried out using a mesh-free particle method. Different numerical test cases are investigated including uni- and bi-directional flow in a passage with and without obstacles.

**keywords:**pedestrian flow models; disease spread models; multi-group macroscopic equations; particle methods

**AMS Subject Classification:**22E46, 53C35, 57S20

## 1 Introduction

The COVID-19 pandemic struck the everyday life worldwide. To avoid further spread in absence of a vaccine or a well-established medical therapy, most countries in the world invoked non-pharmaceutical intervention measures as extensive backtracking, testing and quarantine [21, 12]. One key point is the contact reduction, which is often based on the minimization of the number of contacts and contact time [1, 21, 47]. In many cases, such as in schools or large working facilities social distancing is not always possible, especially at the end of classes or shifts, crowds are formed to leave the facilities. Simulations of disease spread in a moving crowd could give valuable information about how risky these mass events are and support the design of such intervention measures.

Modelling of crowd motion has been investigated in many works on different levels of description. Microscopic (individual-based) models based on Newton type equations as well as vision-based models or cellular automata models and agent-based models have been developed, see Refs. [24, 25, 11, 16, 38, 41]. Associated macroscopic pedestrian flow equations involving equations for density and mean velocity of the flow have been derived as well and investigated thoroughly, see Refs. [6, 38, 23, 20, 2, 13, 14]. An elegant way to include geometrical information and goal of the pedestrians into these models via the additional solution of an eikonal equation has been developed by Hughes, see Refs. [2, 18, 28, 29, 35]. For the derivation and relations of the

above approaches to each other we refer to Refs. [19, 15, 20]. More complex geometries and obstacles have been included into the models by many authors, see, for example, Refs. [41, 45, 46]. Pros and Cons of these models have been discussed in various reviews, we refer to Refs. [6, 26, 3, 7] for a detailed discussion of the different approaches.

On the other hand, there is a vast literature on disease spread models, see Ref. [5] for an overview on multiscale models and connection to crowd dynamics. Moreover, we refer to Refs. [22, 34, 39, 17] for a small selection of papers on mathematical models based on dynamical systems and to Refs. [27, 40, 9] for agent-based and network models. Models coupling crowd motion and contagion dynamics are far less investigated. We refer to Ref. [31] for a recent investigation coupling a crowd motion model with a contagion model in a one-dimensional situation.

One main objective of the present paper is to include a kinetic disease spread model in the form of a multi-group equation into a kinetic pedestrian dynamics model, derive hydrodynamic approximations and provide an efficient numerical simulation of the coupled model for complex two-dimensional geometries. For the pedestrian flow model we consider a kinetic equation for multi-group pedestrian flow based on a social force model coupled with an Eikonal equation to model geometry and goals of the pedestrians. This model is coupled with a non-local contagion model for disease spread, where local contacts as well as the influence of contact times is included. A second objective is the extension of the methodology to situations with more complex geometries and moving objects in the computational domain. This is a way to model, for example, the detailed interaction of pedestrians with larger geometrically extended objects like cars in a shared space environment. See [10] for another approach to the interaction of pedestrians and vehicles. The numerical simulation is, as in Refs. [20, 33], based on mesh-free particle methods [43] for the solution of the Lagrangian form of the hydrodynamic equations. Such a methodology gives an efficient and elegant way to solve the full coupled problem in a complex environment.

The paper is organized in the following way: in section 2 a kinetic model for pedestrian dynamics with disease spread is presented. The section contains also the associated hydrodynamic equations derived from a moment closure approach. The meshfree particle methods used in the simulations is shortly described in Section 3. The section contains also the results of the numerical simulations. The solutions of the macroscopic equations are presented for different physical situations and parameter values including uni-

and bi-directional flow in a two-dimensional passage without obstacles and with fixed and moving obstacles.

## 2 Equations

We use a kinetic model for the evolution of the distribution functions of susceptible, exposed and infected pedestrians as a starting point and derive associated hydrodynamic equations.

### 2.1 Kinetic evolution equation

We consider an equation for the evolution of pedestrian distribution functions  $f^{(k)} = f^{(k)}(x, v, t)$ ,  $k = S, E, I$ . Here  $f^S$  stands for the distribution of susceptible pedestrians,  $f^E$  for the exposed pedestrians and  $f^I$  for the infected. The evolution equations are given by

$$\partial_t f^k + v \cdot \nabla_x f^k + R f^k = T^k \quad (1)$$

with  $k = S, E, I$ . The operators  $R$  and  $T^k$  are given by the following definitions.

$$R f^k(x, v) = \nabla_v \cdot ([G(x, v; \Phi, \rho) - \nabla_x U \star \rho(x)] f^k) .$$

with

$$\rho = \rho^S + \rho^E + \rho^I ,$$

where

$$\rho^k(x) = \int f^k(x, v) dv .$$

Here,  $U$  is an interaction potential describing the local interaction of the pedestrians and  $\star$  denotes the convolution. Common choices for the interaction potential are purely repelling potentials like spring-damper potentials or attractive-repulsive potentials like the Morse potential. In this paper we have, for simplicity, considered a Morse potential without attraction given by

$$U = C_r \exp\left(-\frac{|x - y|}{l_r}\right) , \quad (2)$$

where  $C_r$  is the repulsive strength and  $l_r$  is the length scale. The part of the forcing term involving  $G$  describes the influence of the geometry on the pedestrian's motion and a potential long range interaction between the pedestrians,

see below for a detailed description. The operators  $T^k$  are defined using a SEIS-type kinetic disease spread model leading to

$$\begin{aligned} T^S &= \nu f^I - \beta_I f^S \\ T^E &= \beta_I f^S - \theta f^E \\ T^I &= \theta f^E - \nu f^I \end{aligned} \tag{3}$$

with constants  $\nu, \theta$ , see Remark 3 below, and the non-local infection rate  $\beta_I = \beta_I(x, v; f^S(\cdot), f^E(\cdot), f^I(\cdot))$  depending in a non-local way on the rate of infected persons, compare Refs. [31, 9] for similiar approaches. We define

$$\beta_I = \int \frac{1}{\rho(y)} \int \phi(x - y, v - w) f^I(y, w) dw dy. \tag{4}$$

The kernel  $\phi$  in the infection rate is chosen as

$$\phi = \phi(x, v) = i_o \phi_X(x) \phi_V(v). \tag{5}$$

with  $\int \phi_X(x) dx = 1 = \int \phi_V(v) dv$ . Here,  $\phi_X$  is determined as a decaying function of  $|x|$  to take into account the effect that infections between pedestrians are more probable the closer pedestrians are approaching each other.  $\phi_V$  is chosen in a similar way depending on  $|v|$  to take into account the fact, that infections are more probable the longer the interacting pedestrians stay close to each other, that means the smaller their relative velocities are. The parameter  $i_o$  is determined by the infectivity. We refer to the section on numerical results for the exact definition of these kernels.

Finally,  $G$  is given by

$$G(x, v; \Phi, \rho) = \frac{1}{T} \left( -V(\rho(x)) \frac{\nabla \Phi(x)}{\|\nabla \Phi(x)\|} - v \right), \tag{6}$$

where  $\Phi$  is determined by the coupled solution of the eikonal equation

$$V(\rho) \|\nabla \Phi\| = 1. \tag{7}$$

This describes the tendency of the pedestrians to move with a velocity given by a speed  $V(\rho)$  and a direction given by the solution of the eikonal equation. The eikonal equation essentially includes all information about the boundaries and the desired direction of the pedestrians via the boundary conditions. These boundary conditions for the eikonal equation are chosen

in the following way. For walls or for the boundaries of obstacles in the domain we set the value of  $\Phi$  at the boundary to a numerically large value. For ingoing boundaries, free boundary conditions for  $\Phi$  are chosen, whereas for outgoing boundaries, where the pedestrians aim to go, we set  $\Phi = 0$ .

We note that on the one hand, the eikonal equation includes the geometrical information via boundary conditions. On the other hand, it models a global reaction of the pedestrians to avoid regions of dense crowds via the term  $V(\rho)$  in (7).

**Remark 1.** *The parameters in the above formulas, in particular in the definition of (7) and (2) have to be chosen consistent with empirical data, see [8, 30].*

**Remark 2.** *Instead of the social force model used here, one could as well use more sophisticated interaction models, see for example [16, 4, 36]. We note that the differences between these models in the present hydrodynamic context are small. The behaviour of the solutions is rather dependent on the choice of the parameters.*

**Remark 3.** *The dynamical system called the SEIS-model with constant infection rate is given by*

$$\begin{aligned}\frac{dS}{dt} &= -\beta IS + \nu I \\ \frac{dE}{dt} &= \beta IS - \theta E \\ \frac{dI}{dt} &= \theta E - \nu I\end{aligned}$$

where  $\beta$  is the infection rate,  $\nu$  the recovery rate and  $\theta$  the rate with which exposed persons are becoming infected. Pedestrians are potentially becoming exposed, when they are in contact with infected pedestrians. However, exposed pedestrians are only becoming infectious with a certain rate  $\theta$ . Exposed pedestrians do not infect other pedestrians. Usually, in the situations and on the time scales under consideration here,  $\nu$  and  $\theta$  are very small and set to zero in numerical simulations such that the number of infected pedestrians remains constant during the simulation.

**Remark 4.** *A key difference between other agent-based models as e.g. [9] is the dependence of the infection on the relative velocity of the agents. This has direct implications on the process of infection during the dynamics, as can be seen the the case studies.*

## 2.2 The multi-group hydrodynamic model

Integrating the kinetic equation against  $dv$  and  $vdv$  and using a mono-kinetic distribution function to close the resulting balance equations, i.e. approximate

$$f^k \sim \rho^k(x) \delta_{u(x)}(v)$$

one obtains a continuity equation for group  $k$

$$\partial_t \rho^k + \nabla_x \cdot (\rho^k u) = \int T^k dv \quad (8)$$

and the momentum equation

$$\partial_t u + (u \cdot \nabla_x) u = G(x, u; \Phi, \rho) - \nabla_x U \star \rho \quad (9)$$

with the total density  $\rho$  given as

$$\rho = \rho^S + \rho^E + \rho^I.$$

Moreover,

$$G(x, u; \Phi, \rho) = \frac{1}{T} \left( -V(\rho(x)) \frac{\nabla \Phi(x)}{\|\nabla \Phi(x)\|} - u \right),$$

where  $\Phi$  is determined by solving the eikonal equation

$$V(\rho) \|\nabla \Phi\| = 1.$$

The continuity equations are explicitly written as

$$\begin{aligned} \partial_t \rho^S + \nabla_x \cdot (u \rho^S) &= \nu \rho^I - \beta_I \rho^S \\ \partial_t \rho^E + \nabla_x \cdot (u \rho^E) &= \beta_I \rho^S - \theta \rho^E \\ \partial_t \rho^I + \nabla_x \cdot (u \rho^I) &= \theta \rho^E - \nu \rho^I. \end{aligned} \quad (10)$$

with  $\beta_I = \beta_I(x; \rho^S(\cdot), \rho^E(\cdot), \rho^I(\cdot), u(\cdot))$ , where now

$$\beta_I = \int \phi(x - y, u(x) - u(y)) \frac{\rho_I(y)}{\rho(y)} dy. \quad (11)$$

**Remark 5.** *Multi-group models for pedestrian flows have been also used in different contexts. For example in [37] a hydrodynamic multi-group model for pedestrian dynamics with groups of different sizes has been developed and analysed in [37].*

## 2.3 The hydrodynamic model using volume fractions

For numerical computations this is rewritten using volume fractions, that means we solve the continuity equation

$$\partial_t \rho + \nabla_x \cdot (\rho u) = 0 \quad (12)$$

and the momentum equation

$$\partial_t u + (u \cdot \nabla_x) u = G(x, u; \Phi, \rho) - \nabla_x U \star \rho. \quad (13)$$

Then we compute the volume fractions  $\alpha^S, \alpha^E, \alpha^I$  with  $\alpha^S + \alpha^E + \alpha^I = 1$  as

$$\begin{aligned} \partial_t \alpha^S + u \cdot \nabla_x \alpha^S &= \nu \alpha^I - \beta^I \alpha^S \\ \partial_t \alpha^E + u \cdot \nabla_x \alpha^E &= \beta^I \alpha^S - \theta \alpha^E \\ \partial_t \alpha^I + u \cdot \nabla_x \alpha^I &= \theta \alpha^E - \nu \alpha^I \end{aligned} \quad (14)$$

with  $\beta_I = \beta_I(x; \alpha^I(\cdot), u(\cdot))$  defined by

$$\beta_I = \int \phi(x - y, u(x) - u(y)) \alpha_I(y) dy. \quad (15)$$

Finally, one computes

$$\rho^I = \alpha^I \rho, \rho^S = \alpha^S \rho, \rho^E = \alpha^E \rho.$$

## 2.4 Dynamic geometries

We allow the domain on which the above equations are defined to depend on time. In particular, we consider moving obstacles, which change their path and speed in order to avoid collisions with the pedestrians, while moving towards a specific target. The interaction between the pedestrians and the moving obstacle is additionally modeled by kinematic equations using a repulsive potential similar to the pedestrian-pedestrian interactions. A second Eikonal equation is integrated for modelling the path of the moving obstacle in the geometry and the desired destination of the obstacle. The velocity update equation for the obstacle is given as

$$\frac{dx^O}{dt} = v^O,$$

$$\frac{dv^O}{dt} = -\nabla_x U^O * \rho(x^O) + G^O(x^O, v^O; \Phi^O, \rho), \quad (16)$$

where  $x^O$  and  $v^O$  are the position and velocity of the obstacle's centre of mass,  $\rho$  is the density of pedestrians at  $x^O$ .  $U^O$  is an interaction potential describing the interaction of the pedestrians on the obstacle.

$G^O$  is obtained from the gradient of the Eikonal solution  $\phi_O$  for the obstacle as

$$G^O(x^O, v^O; \Phi^O, \rho) = -\frac{1}{T^O} \left( -V^O(\rho(x^O)) \frac{\nabla \phi^O(x^O)}{\|\nabla \phi^O(x^O)\|} - v^O \right), \|\nabla \phi^O\| = 1.$$

That means, the eikonal equation is for the obstacle only used to include the geometrical informations and the goal of the obstacle. We note that the action of the obstacle on the pedestrians is given by the solution of equation (7) via the boundary conditions at the obstacle's boundaries. In contrast, the action of the pedestrians on the obstacle is given via  $U^O$ .

### 3 Numerical method and results

For the numerical simulation we use a meshfree particle method, which is based on least square approximations. [44, 33] A Lagrangian formulation of the hydrodynamic equations is used and coupled to the SEIS model and the obstacle's kinematic equations Eq. (16).

#### 3.1 Lagrangian equations

The spatially discretized system in Lagrangian form is given by

$$\begin{aligned} \frac{dx_i}{dt} &= u_i, \\ \frac{d\rho_i}{dt} &= -\rho_i \nabla_x \cdot u_i, \\ \frac{du_i}{dt} &= G(x_i, u_i; \Phi, \rho) - \sum_j \nabla U(x_i - x_j) \rho_j dV_j, \end{aligned} \quad (17)$$

and

$$\frac{d\alpha_i^S}{dt} = \nu \alpha_i^I - \beta_i^I \alpha_i^S \quad (18)$$

$$\frac{d\alpha_i^E}{dt} = \beta_i^I \alpha_i^S - \theta \alpha_i^E \quad (19)$$

$$\frac{d\alpha_i^I}{dt} = \theta \alpha_i^E - \nu \alpha_i^I \quad (20)$$

with

$$\beta_i^I = \sum_j \phi(x_i - x_j, u_i - u_j) \alpha_j^I dV_j,$$

and

$$\begin{aligned} \frac{dx^O}{dt} &= v^O, \\ \frac{dv^O}{dt} &= G^O(x^O, v^O; \Phi^O, \rho) - \sum_j \nabla U^O(x^O - x_j) \rho_j dV_j. \end{aligned} \quad (21)$$

Here  $dV_j$  is the local area around a particle.

**Remark 6.** *Although the equations in Lagrangian form look similar to a microscopic problem, there are important differences. In particular, the efficient solution of the continuity equation (compared to a determination of the density in a purely microscopic simulation) and the consequent availability of  $\rho_i$  on each grid-point allows the efficient use of the density, used at various places in the model.*

### 3.2 Numerical method

For a description of the mesh-free method for the pedestrian flow equations in a fixed rectangular domain, we refer to [43, 33]. There, the eikonal equation has been solved on a separate regular mesh on the entire domain using the fast-marching method. The information from the irregular point cloud, used for solving the fluid equations has been interpolated to the eikonal grid and vice versa. Such an approach requires for a moving obstacle to take special care of the grid points being overlapped by the obstacles. Using an immersed boundary method, they are activated and deactivated depending on the location of the obstacle.

Here, we have followed a different approach. The eikonal equation is directly solved on the irregular point cloud used for the hydrodynamic equations. Thus, in each time step an eikonal equation on an unstructured grid has to be solved, see [42] for the Fast-marching method in this case. The

approximation of the spatial derivatives in the eikonal equation is obtained as for the hydrodynamic equations: the spatial derivatives at an arbitrary grid point are computed from the values at its surrounding neighboring grid points using a weighted least squares method. We refer to [32] for a numerical study of the accuracy and complexity of such a method for the eikonal equation.

Finally, we note that for a uni-directional flow of pedestrians, we have to solve only one eikonal equation. If there is bi-directional flow, we have to solve an eikonal equation for each direction. The same would be true for several obstacles with different goals.

### 3.3 Numerical results

We have performed numerical simulations of equations (Eq. (12) to Eq. (15) and (16) for different scenarios. In all our simulations, we consider a computational domain given by a platform or corridor of size  $100\text{ m} \times 50\text{ m}$ . The top and bottom boundaries are rigid walls without any entry or exit. Right and left boundary are exits for pedestrians and obstacles depending on the situation under consideration. We consider uni- as well as bi-directional flow of the pedestrians. Initially, the pedestrians are distributed as shown in Figure 1 with a distance of  $1.575\text{ m}$  from each other. We consider the cases with and without obstacles, which are either fixed or moving. We initialize the infected pedestrians (colored in red) with  $\alpha_I = 1, \alpha_S = 0, \alpha_E = 0$ , the susceptibles (in green) by  $\alpha_I = 0, \alpha_S = 1, \alpha_E = 0$ .

We have used for the infection rate  $\beta_I$  the functions  $\phi_X = \exp(-|x - y|^4)$  and  $\phi_V = \exp(-|u - v|^6)$ . Moreover, we choose  $V(\rho) = V_{max} \left(1 - \frac{\rho}{\rho_{max}}\right)$  and  $V^O(\rho)$  in the same way with  $V_{max}$  substituted by  $V_{max}^O$ . For the parameters we have used the values given in Table 1.

Variable	Value	Variable	Value
$V_{max}$	$2\text{ m/s}$	$\rho_{max}$	$10\text{ ped/m}^2$
$V_{max}^O$	$3\text{ m/s}$	T	$0.001\text{ s}$
$C_r = C_r^O$	50	$l_r$	2 m
$l_r^O$	1 m	$i_o$	$0.04\text{ m}^2/\text{s}^2$

Table 1: Numerical parameters.

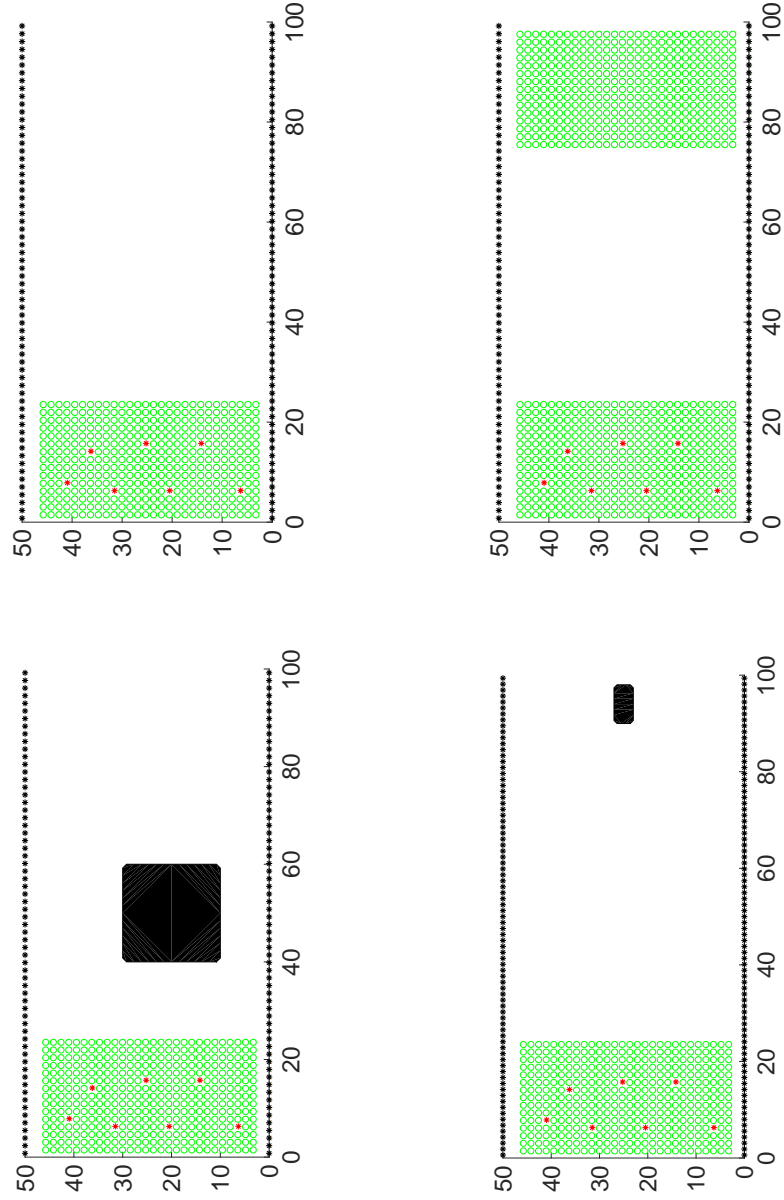


Figure 1: Initial situation at  $t = 0$ . Top row: Uni-directional (left) and bi-directional (right) flow. Bottom row: Fixed obstacle (left) and moving obstacle (right). Red indicate infected, green indicate susceptible pedestrians.

During the evolution, infected pedestrians are colored in red, susceptibles in green and exposed pedestrians in blue according to the values of  $\alpha^k$ . If  $\alpha^E > 0.05$  the colour is switching from green to blue, meaning that the probability of being exposed has exceeded a certain threshold. The red pedestrians remain red throughout the simulations, since the recovery rate  $\nu$  is set equal to 0 in the simulations. Moreover, since  $\theta$  is also set to 0 exposed patients are not becoming infected and cannot infect others in the simulations.

The fixed and the moving obstacle considered are rectangular in shape and initially located as shown in Figure 1.

Explicit time integration of the equations in Lagrangian form is done with a fixed time step size of 0.001 in our simulations.

### 3.4 Test-case 1: fixed obstacle

In this first test case we have considered a fixed obstacle and compared the results to a situation without obstacle. We consider bi-directional flow without an obstacle and uni- and bi-directional flow with an obstacle. This is done for the case  $\phi_v = 0$  (no influence of contact time) and the case where  $\phi_V$  is chosen as defined above, that means for a situation where the influence of the contact time is included. The present initial configuration is chosen in such a way, that there is no increase of the number of probably exposed pedestrians, if a uni-directional flow without obstacle is considered with or without influence of the contact time.

Figures 2 to 5 show the time evolution of the moving grid points and the associated infection labels with influence (left column) and without influence (right column) of contact time. Row 1 shows bi-directional flow without an obstacle, row 2 shows uni-directional flow around an obstacle and row 3 shows bi-directional flow around an obstacle. Red indicate infected, green indicate susceptibles and blue indicate exposed pedestrians.

Here one observes, e.g. in Figure 4 or 5, that in situations with bi-directional flow (top- and bottom row), the number of exposed patients is strongly reduced, if the contact time is taken into account. For uni-directional flow, the differences are much smaller as expected, since pedestrians stay near to each other for a longer time during the evolution.

Comparing row 2 (uni-directional with obstacle) with the uni-directional case without obstacle (no exposed pedestrians), one observes that the number of exposed patients is considerably increased due to the denser pedestrian crowd surrounding the obstacle. Similar observations can be made comparing

row 1 and row 3.

In Figure 6 we have plotted the number of pedestrians with a higher probability of being exposed versus time. One can observe, that the number of these pedestrians is much higher if the influence of the contact time is neglected. This happens mainly in bi-directional flows, which is as expected, since, even if pedestrians are coming close to each other, they pass each other quickly and the contact time is short such that a contagion is less probable. On the other hand if pedestrians are walking in the same direction, the effect of neglecting the contact time is comparably small. We mention, that the contagion model is based on very simple assumptions and obviously the parameters of the contagion model have to be adapted to experimental findings. We refer again to [31] for similiar investigations.

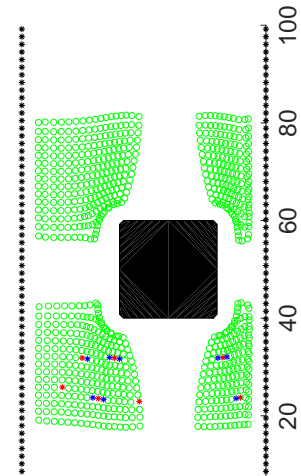
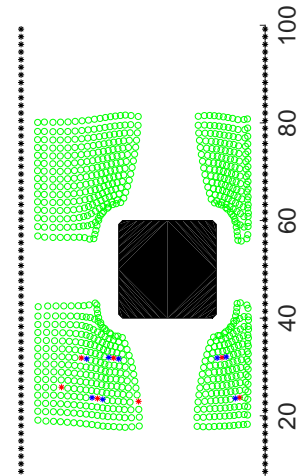
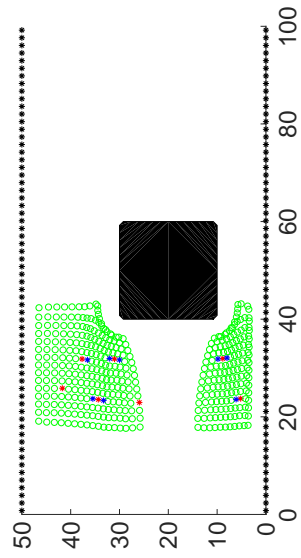
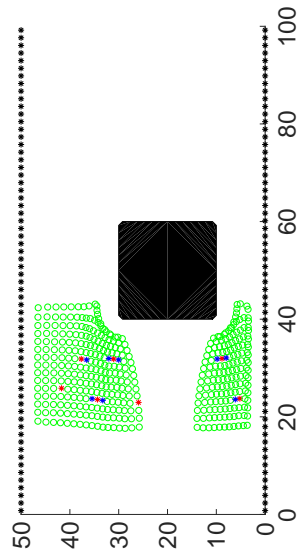
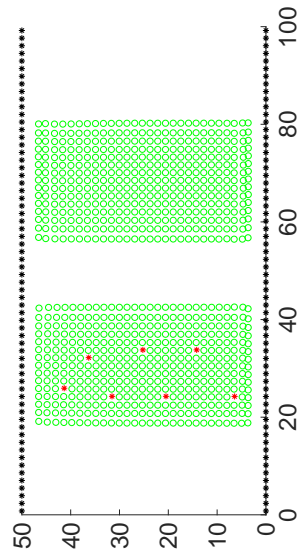
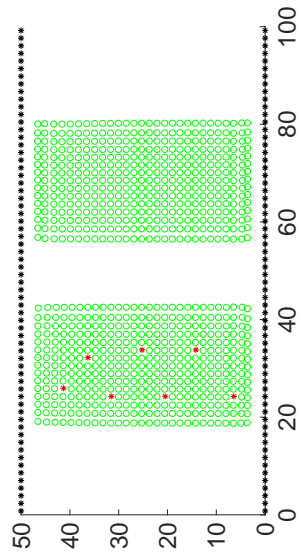
Finally, in Figure 7 we show the macroscopic density of the pedestrians at times  $t = 10, 20, 30, 40$  for the situation with influence of contact time for uni-directional flow with fixed obstacle.

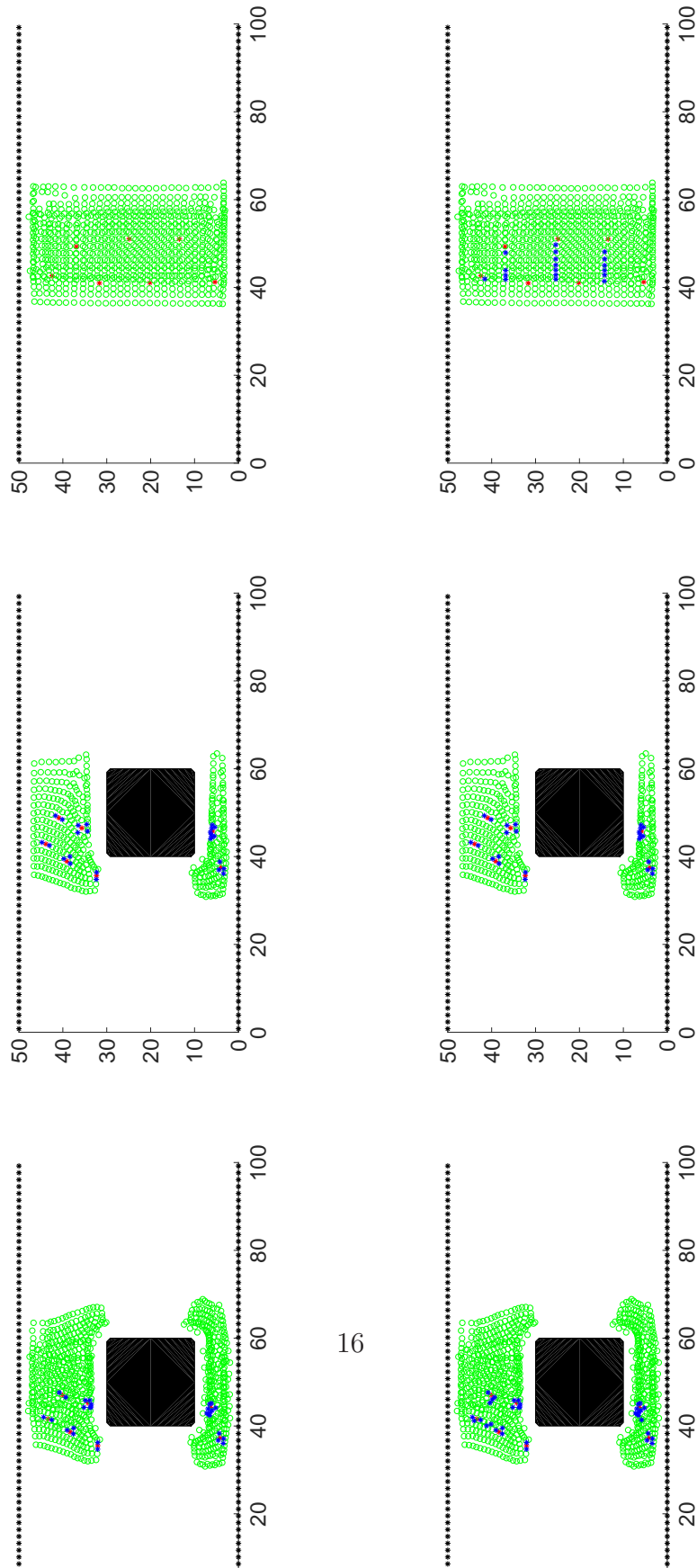
### 3.5 Test-case 2: moving obstacle

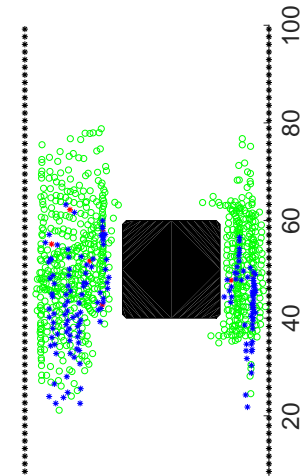
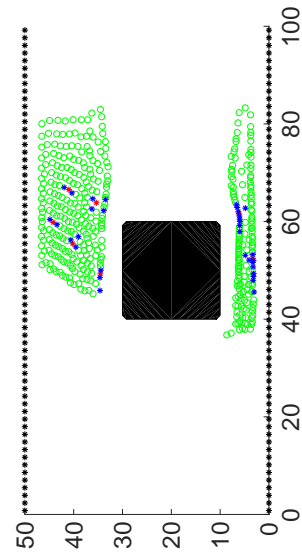
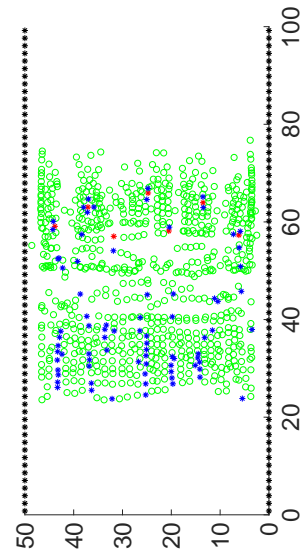
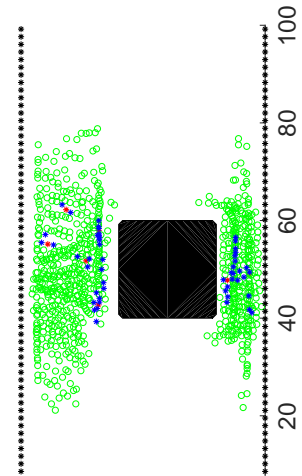
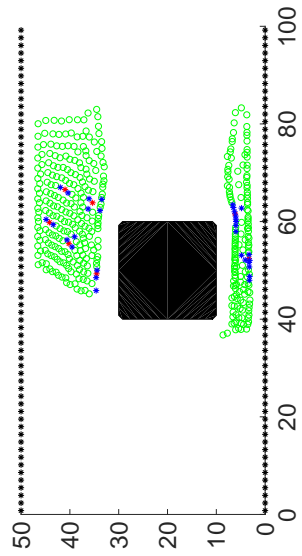
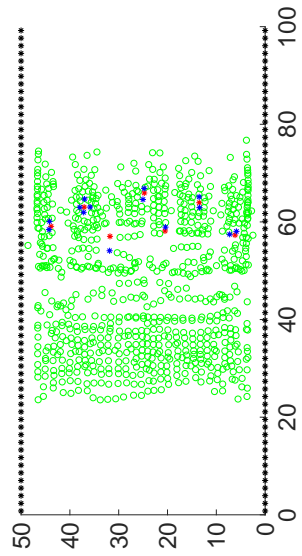
In this subsection we consider the interaction of pedestrians with a moving obstacle, e.g. a vehicle in a shared space. We consider the same computational domain as in test-case 1 with pedestrians, which are initially located as in Figure 1 (right bottom). Their destination is the right exit. The moving obstacle of size  $4m \times 8m$  is located on the right with the left exit as destination. Typically in a restricted traffic area the vehicle has a low speed limit. We have chosen  $10km/h \sim 3m/s$ . The maximum speed of the pedestrians is chosen as  $2m/s$ .

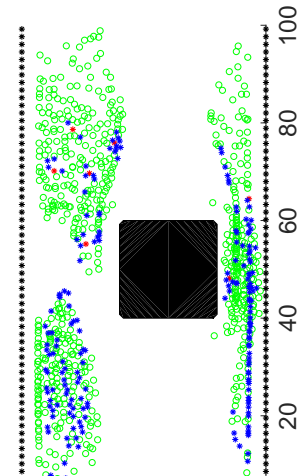
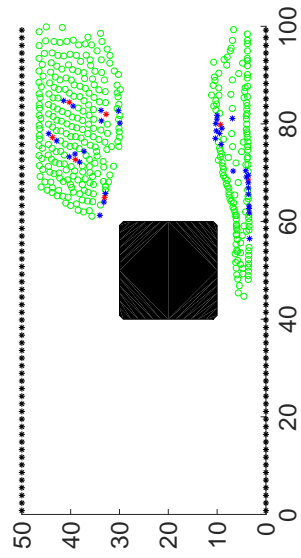
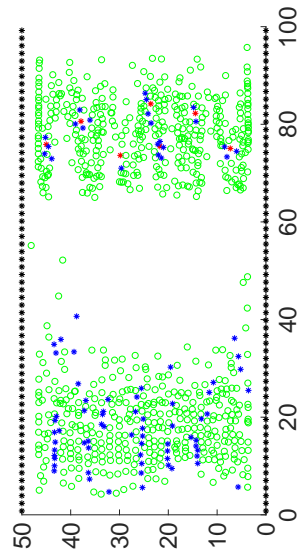
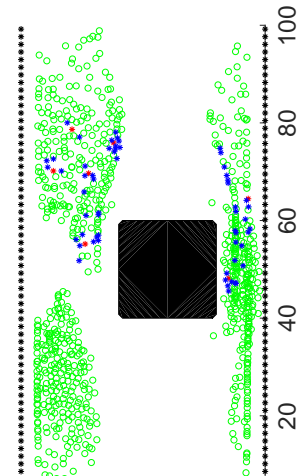
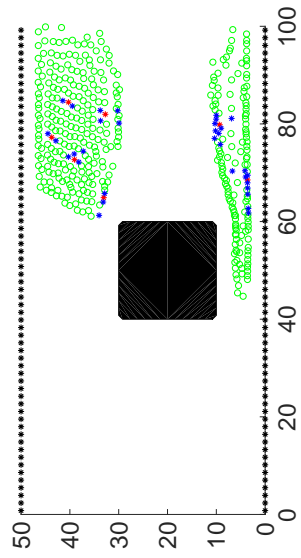
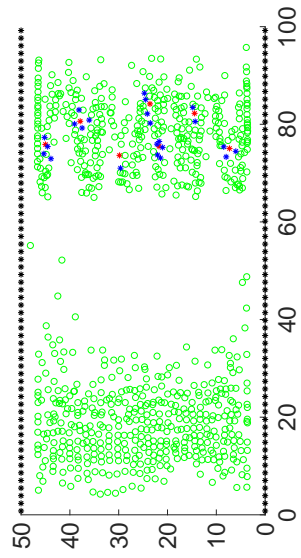
In Figure 8 we have plotted the positions of pedestrians and obstacle at different times  $t = 8s, 14s, 18s$  and  $22s$ . We observe an interaction of pedestrians and obstacle between times  $t = 14s$  and  $t = 22s$ . Moreover, one observes a slight increase of the number of exposed people which is less pronounced than in the case of the big fixed obstacle in test-case 1.

Moreover, in Figure 9 we have plotted the  $x$ -velocity component of the obstacle along its center of mass. One observes that the obstacle (coming from the right) accelerates and maintains almost its maximum speed. When it encounters the pedestrian crowd, it reduces its speed. Finally, it accelerates again, when there are no pedestrians anymore in the surroundings.









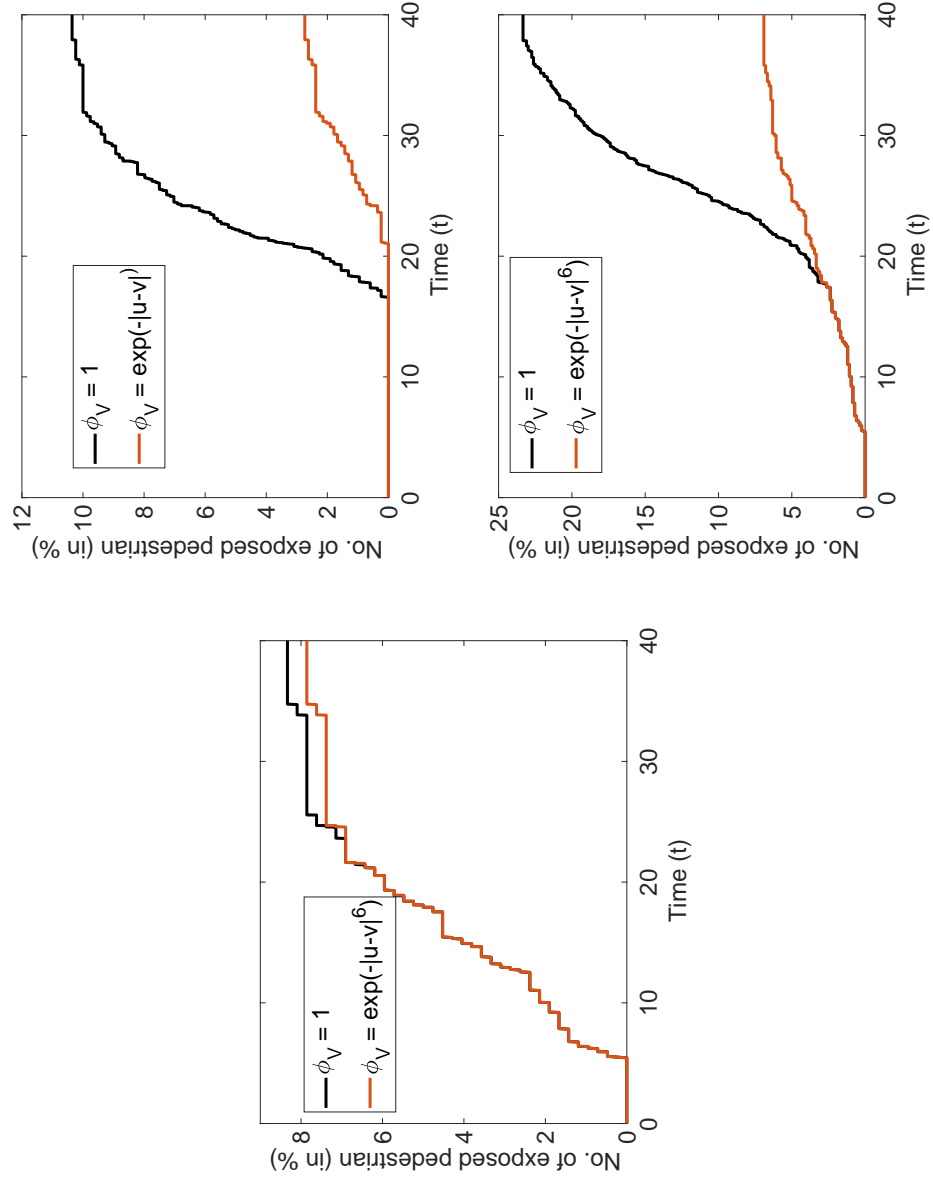


Figure 6: Number of pedestrian with an increased probability of being exposed (in %) vs time. First row bi-directional flow without obstacle (left) and with obstacle (right). Second row: uni-directional with obstacle.

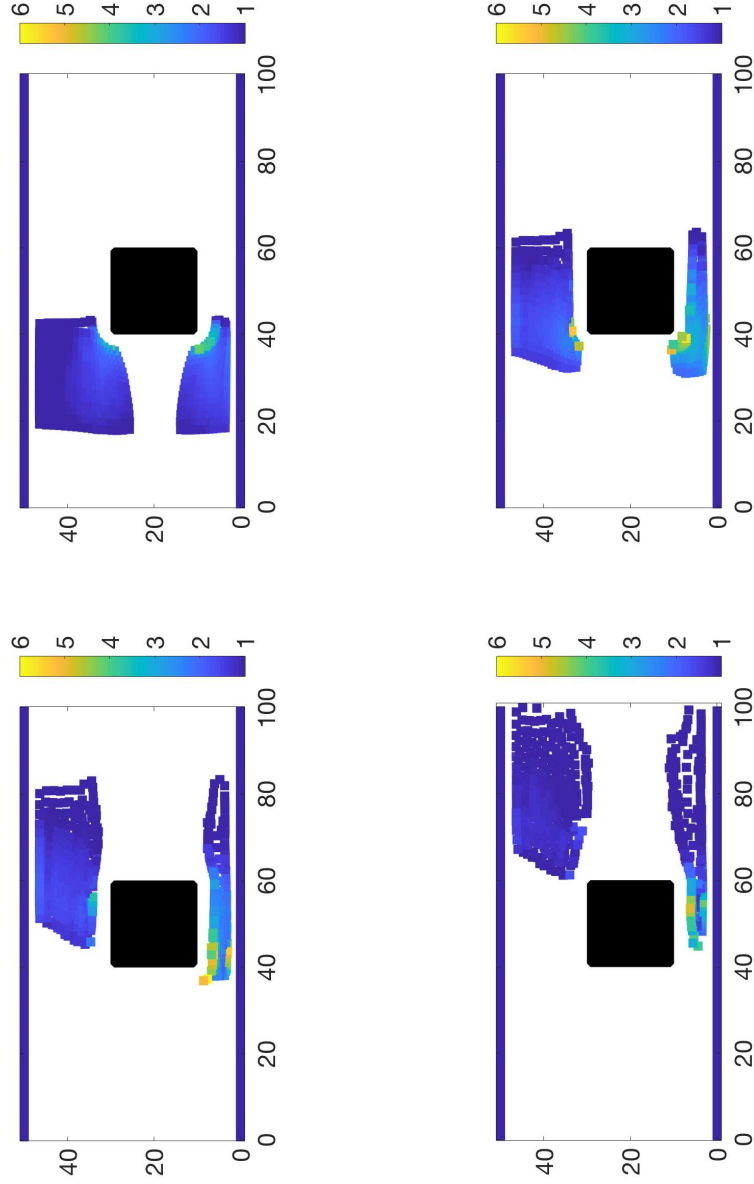


Figure 7: Macroscopic density  $\rho$  of pedestrian dynamics at times  $t = 10, 20, 30, 40$  with influence of contact time for uni-direction flow with fixed obstacle.

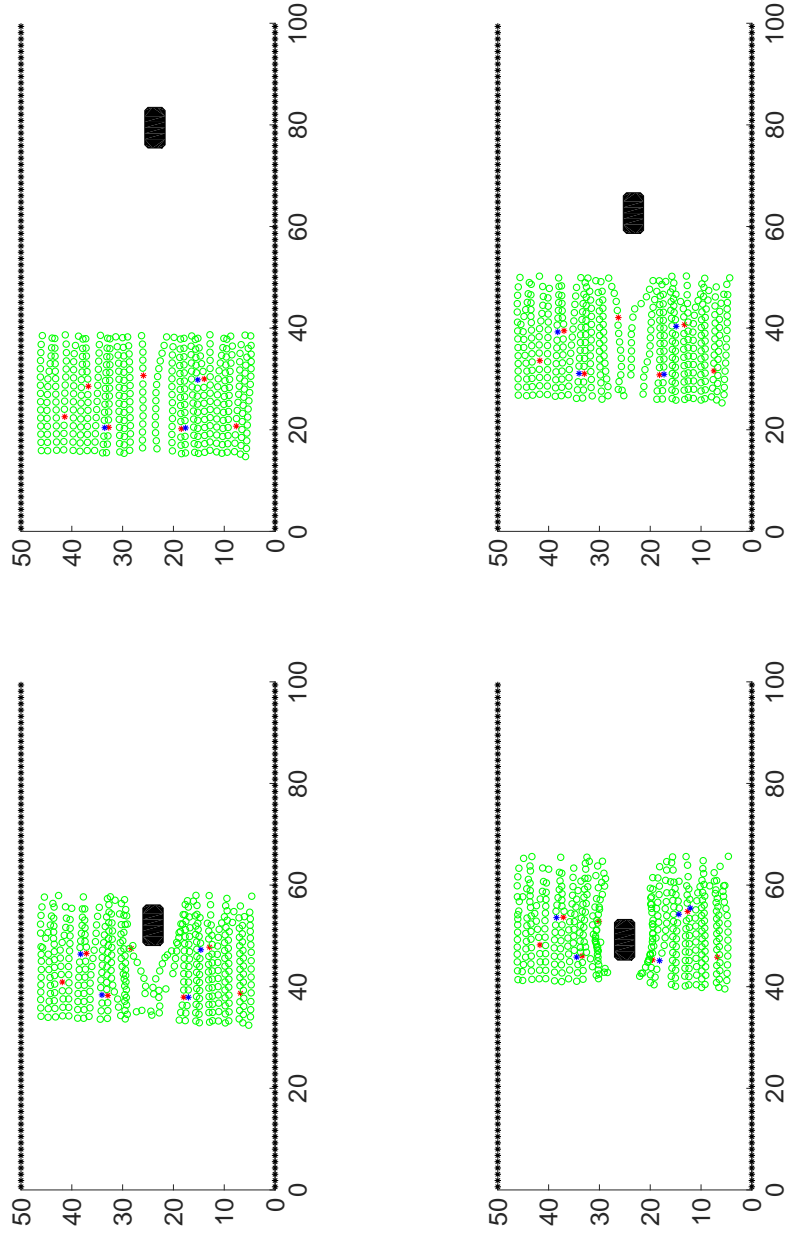


Figure 8: Positions of pedestrian and obstacle at  $t = 8s, 14s$  (first row) and  $t = 18s, 22s$  (second row). Red indicate infected, green indicate susceptibles, blue indicate probably exposed pedestrians.

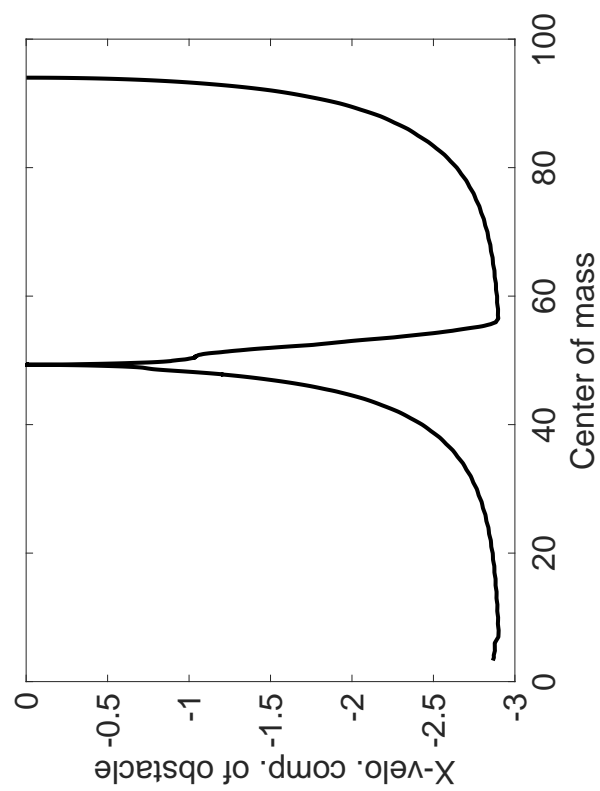


Figure 9: The velocity of the obstacle along the center of mass.

## 4 Concluding Remarks

We have presented a multi-group macroscopic pedestrian flow model combining a dynamic model for pedestrians flows and a SEIS based kinetic disease spread model. A meshfree particle method to solve the governing equations is presented and used for the computation of several numerical examples analyzing different situations and parameters. The dependence of the solutions and, in particular, the dependence of the number of exposed pedestrians on geometry and parameters is investigated and discussed and shows qualitatively consistent results. Findings indicate, that in particular, in bi-directional flow it is important to take into account the contact time for a realistic description of the flow. This is a realistic qualitative behavior, which sheds a new light for the design of emergency exits in the presence of a pandemic.

## Acknowledgment

This work is supported by the German research foundation, DFG grant KL 1105/30-1 and by the DAAD PhD program MIC.

## References

- [1] B. Adamik, M. Bawiec, V. Bezborodov, W. Bock, M. Bodych , J. Burgard, ... & T. Ozanski, (2020). *Mitigation and herd immunity strategy for COVID-19 is likely to fail*. medRxiv (preprint) Available at: <https://doi.org/10.1101/2020.03.25>.
- [2] D. Amadoria and M. Di Francesco, *The one-dimensional Hughes model for pedestrian flow: Riemann-type solutions*, Acta Math. Sci. 32 (2012) 259-280.
- [3] G. Albi, N. Bellomo, L. Fermo, S.-Y. Ha, J. Kim, L. Pareschi, D. Poyato, and J. Soler, *Traffic, crowds, and swarms. From kinetic theory and multiscale methods to applications and research perspectives*, Math. Models Methods Appl. Sci., 29, (2019), 1901-2005.
- [4] R. Bailo, J. A. Carrillo, P. Degond, *Pedestrian Models based on Rational Behaviour*, <https://arxiv.org/abs/1808.07426>

- [5] N. Bellomo, R. Bingham, M. A. J. Chaplain, G. Dosi, G. Forni, D. A. Knopoff, J. Lowengrub, R. Twarock, and M. E. Virgillito, *A multi-scale model of virus pandemic: Heterogeneous interactive entities in a globally connected world*, Math. Models Methods Appl. Sci., doi: 10.1142/S0218202520500323.
- [6] N. Bellomo and C. Dogbe, *On the modeling of traffic and crowds: A survey of models, speculations, and perspectives*, SIAM Rev. 53 (2011) 409-463.
- [7] N. Bellomo, A. Bellouquid, D. Knopoff, *From the microscale to collective crowd dynamics*, SIAM J. Multiscale Model. Simul. 11 (2013) 943–963.
- [8] N. Bellomo, L. Gibelli, and N. Outada, *On the Interplay between Behavioral Dynamics and Social Interactions in Human Crowds*, Kinetic Related Models, 12, (2019), 397-409, (2019).
- [9] W. Bock, T. Fattler, I. Rodiah, and O.Tse. *An analytic method for agent-based modeling of spatially inhomogeneous disease dynamics*. In AIP Conference Proceedings (Vol. 1871, No. 1, p. 020008). AIP Publishing LLC. 2017.
- [10] R. Borsche, A. Klar, S. Kühn, A. Meurer, *Coupling traffic flow networks to pedestrian motion*, Math. Methods Models Appl. Sci. 24, 2, 359-380, 2014
- [11] C. Burstedde, K. Klauck, A. Schadschneider, J. Zittartz, *Simulation of pedestrian dynamics using a two-dimensional cellular automaton*, Physica A 295 507–525, 2001.
- [12] R.Chowdhury, K.Heng, M. S. R. Shawon, G. Goh, D. Okonofua, C. Ochoa-Rosales, ... & S. Shahzad (2020). *Dynamic interventions to control COVID-19 pandemic: a multivariate prediction modelling study comparing 16 worldwide countries*. European journal of epidemiology, 35(5), 389-399.
- [13] R. Colombo, M. Garavello, M. Lecureux-Mercier, *A Class of Non-Local Models for Pedestrian Traffic*, Math. Models Methods Appl. Sci. 22 (2012) 1150023.

- [14] R. Colombo, M. Garavello, M. Lecureux-Mercier, *Non-local crowd dynamics*, Comptes Rendus Mathematique 349 (2011) 769–772.
- [15] E. Cristiani, B. Piccoli, and A. Tosin, Multiscale Modeling of Pedestrian Dynamics, Springer, (2014).
- [16] P. Degond, C. Appert-Rolland, M. Moussaid, J. Pettre and G. Theraulaz, *A hierarchy of heuristic-based models of crowd dynamics*, J. Stat. Phys. 152 (2013) 1033-1068.
- [17] Dessalegn Y. Melesse, Abba B. Gumel, *Global asymptotic properties of an SEIRS model with multiple infectious stages*, J. Math. Anal. Appl. 366 (2010) 202–217.
- [18] M. Di Francesco, P.A. Markowich, J.F. Pietschmann and M.T. Wolfram, *On the Hughes model for pedestrian flow: The one-dimensional case*, J. Differential Equations 250 (2011) 1334-1362.
- [19] M. Di Francesco, S. Fagioli, M.D. Rosini, G. Russo, *Deterministic particle approximation of the Hughes model in one space dimension*, Kinetic and Related Models, 10, 1, (2017), 215–237
- [20] R Etikyala, S Göttlich, A Klar, and S Tiwari. *Particle methods for pedestrian flow models: From microscopic to nonlocal continuum models* Mathematical Models and Methods in Applied Sciences, 20(12), 2503–2523, 2014.
- [21] N.M.Ferguson , D. Laydon, G. Nedjati-Gilani, et al. *Impact of non-pharmaceutical interventions (NPIs) to reduce COVID19 mortality and healthcare demand*. London: WHO Collaborating Centre for Infectious Disease Modelling MRC Centre for Global Infectious Disease Analysis Abdul Latif Jameel Institute for Disease and Emergency Analytics Imperial College London; 2020.
- [22] Herbert W. Hethcote, *The Mathematics of Infectious Diseases*, SIAM REVIEW Vol. 42, No. 4, pp. 599–653, 2000
- [23] D. Helbing, *A fluid dynamic model for the movement of pedestrians*, Complex Syst. 6 (1992) 391-415.

- [24] D. Helbing and P. Molnar, *Social force model for pedestrian dynamics*, Phys. Rev. E, 51 (1995), pp. 4282-4286.
- [25] D. Helbing, I.J. Farkas, P. Molnar, and T. Vicsek, *Simulation of pedestrian crowds in normal and evacuation situations*, in: *M. Schreckenberg, S.D. Sharma(Eds.)*, Pedestrian and Evacuation Dynamics, Springer-Verlag, Berlin, 2002, pp. 21-58.
- [26] D. Helbing, A. Johansson, *Pedestrian, Crowd and Evacuation Dynamics*. Encyclopedia of Complexity and Systems Science 16, (210), 6476-6495.
- [27] T. House, *Modelling epidemics on networks*. Contemporary Physics, 53(3), pp.213-225, 2012.
- [28] R.L. Hughes, *A continuum theory for the flow of pedestrians*, Transp. Res. Part B: Methodological 36 (6) (2002), pp. 507-535.
- [29] R.L. Hughes, *The flow of human crowds*, Ann. Rev. Fluid Mech. 35 (2003) 169-182.
- [30] D.P. Kennedy, J. Gläscher, J.M. Tyszka, R. Adolphs, *Personal space regulation by the human amygdala*. Nat Neurosci. 12, 1226–1227, 2009.
- [31] D. Kim and A. Quaini, *Coupling kinetic theory approaches for pedestrian dynamics and disease contagion in a confined environment*, Math. Models Methods Appl. Sci., 30(9), (2020).
- [32] A. Klar, S. Tiwari, and E. Raghavender, *Mesh Free method for Numerical Solution of The Eikonal Equation*, *Proceedings of International workshop on PDE Modelling and Computation*, Advances in PDE Modelling and Computation, Ane Books Pvt. Ltd., 2013.
- [33] A. Klar, S. Tiwari, *A multi-scale particle method for mean field equations: the general case*, SIAM Multiscale Mod. Simul. 17 (1), 233-259, 2019
- [34] Andrei Korobeinikov, *Lyapunov functions and global properties for SEIR and SEIS epidemic models*, Mathematical Medicine and Biology, 2004

- [35] H. Ling, S.C. Wong, M. Zhang, C.H. Shu, and W.H.K. Lam, *Revisiting Hughes dynamics continuum model for pedestrian flow and the development of an efficient solution algorithm*, Transp. Res. Part B: Methodological, 43 (1) (2009), pp. 127-141.
- [36] N. K. Mahato, A. Klar, S. Tiwari, *A meshfree particle method for a vision-based macroscopic pedestrian model*, Int. J. Adv. Eng. Sci. Appl.Math 10, 1, 41-53, 2018
- [37] N.K. Mahato, A. Klar, S. Tiwari, *Particle methods for multi-group pedestrian flow*, Appl. Math. Modeling 53, 447-461, 2018
- [38] B. Maury, A. Roudneff-Chupin and F. Santambrogio, *A macroscopic crowd motion model of the gradient-flow type*, Math. Models Methods Appl. Sci. 20 (2010) 1787-1921.
- [39] Suzanne M. O'Regan, Thomas C. Kelly, Andrei Korobeinikov, Michael J.A. O'Callaghan, Alexei V. Pokrovskii, *Lyapunov functions for SIR and SIRS epidemic models*, AppliedMathematicsLetters23, 446-448, 2010
- [40] L. Perez, & S. Dragicevic, *An agent-based approach for modeling dynamics of contagious disease spread*. International journal of health geographics, 8(1), 50, 2009.
- [41] B. Piccoli and A. Tosin, *Pedestrian flows in bounded domains with obstacles*, Contin. Mech. Thermodynam. 21 (2009) 85-107.
- [42] J.A. Sethian, *Fast marching methods*, SIAM Rev. 41 (1999) 199-235.
- [43] S. Tiwari, and J. Kuhnert, *Finite pointset method based on the projection method for simulations of the incompressible Navier-Stokes equations*, Meshfree Methods for Partial Differential Equations, eds. M. Griebel and M.A. Schweitzer, Lecture Notes in Computational Science and Engineering, Vol. 26 (Springer-Verlag, 2003), pp. 373-387.
- [44] S. Tiwari, and J. Kuhnert, *Modelling of two-phase flow with surface tension by finite pointset method(FPM)*, J. Comp. Appl. Math, 203 (2007), pp. 376-386.
- [45] M. Twarogowska, P. Goatin, R. Duvigneau, *Macroscopic modeling and simulations of room evacuation*, Applied Mathematical Modelling, 38, Issue 24, 2014, 5781-5795

- [46] A. Treuille, S. Cooper, Z. Popovic, *Continuum crowds*, in: *ACM Transaction on Graphics*, Proceedings of SCM SIGGRAPH 25 (2006) 1160–1168.
- [47] P.G. Walker, C. Whittaker, O. Watson, et al. *The global impact of COVID-19 and strategies for mitigation and suppression*. London: WHO Collaborating Centre for Infectious Disease Modelling, MRC Centre for Global Infectious Disease Analysis, Abdul Latif Jameel Institute for Disease and Emergency Analytics, Imperial College London; 2020.